Available online at www.sciencedirect.com

SCIENCE DIRECT

Journal of Sound and Vibration 284 (2005) 583–595

JOURNAL OF SOUND AND VIBRATION

www.elsevier.com/locate/jsvi

A non-standard analysis approach to systems involving friction

Naser Mostaghel*

Department of Civil Engineering, University of Toledo, Toledo, OH 43606, USA

Received 25 February 2004; accepted 24 June 2004
Available online 19 November 2004

Abstract

Many physical systems involve discontinuous forces. The conventional numerical discretization approach does not always yield a consistent prediction of the behavior of these systems. Here, as an example of a system involving discontinuous forces, a simple frictional system subjected to continuous as well as discontinuous excitations is considered. A set of orthogonal tracking functions is introduced, and the discontinuous excitation is expanded in a series of these tracking functions. Using non-standard analysis, the discontinuous functions are rigorously represented by continuous hyperreal approximations. The transformation of discontinuous forces to continuous ones allows consistent prediction of the system's behavior, thus providing a reliable technique for simulation of systems involving discontinuous forces.

1. Introduction

In many mechanical systems such as sliding seismic isolators [1–6], turbo machinery, and space structures, friction is the main source of damping. Friction can give rise to self-sustained oscillations resulting in undesirable behaviors such as *machine tool chattering,* which increases tool wear and reduces production quality, and high-frequency noise "*squeal*" induced by nonlinear slip forces in wheels, which in vehicles is quite annoying to both occupants and passersby. It is also a major problem in feedback control applications and is the main source of jerky or hunting motions about the desired positions of robotic systems [7–10]. Coulomb friction is widely used in numerical simulation of these systems. Even this simple model involves considerable complexities

*Tel.: +1 419 5308131; fax: +1 419 5308116.
E-mail address: nmostag@utnet.utoledo.edu (N. Mostaghel).

doi:10.1016/j.jsv.2004.06.041

for analysis. The friction force is a discontinuous function of velocity and the coefficient of friction is itself a function of velocity. Because of discontinuous physical effects, the conventional numerical simulation methods, which treat such discontinuities with discretized representations, do not always provide a consistent description of the behavior of systems with discontinuous forces, and can lead to erroneous results.

Rzymowski [11] has proved the existence of solutions for the class of discontinuous dynamic systems that includes dynamic frictional systems. According to Filippov [12], the evaluation of the correct solutions of dynamical systems involving discontinuous forces by well-known methods requires that the limit of a uniformly convergent sequence of solutions itself be a solution. He has developed an algorithm by which the discontinuous system is approximated by a continuous one after a regularization process. Danca and Coreanu [13] have explored the possibility of directly approximating the discontinuous systems with continuous ones, eliminating the regularization process.

A newly evolving field in calculus is the field of non-standard analysis (NSA), which has provided the rigorous basis for calculus. NSA was conceived in the early 1960s by Robinson [14]. Keisler [15] has published a very good textbook on the subject. In NSA, the real line R is extended to a hyperreal line $^*R$, which contains infinite numbers as well as infinitesimals. A hyperreal number x is considered as finite if $|x| \prec n$. And x is considered as infinitesimal if $|x| \prec 1/n$ for all integers n. It is noted that 0 is trivially infinitesimal. The difference between the hyperreal and the real lines is that the hyperreal line contains an infinite H and an infinitesimal $\varepsilon = 1/H$. To visualize a physical meaning for hyperreal quantities, Keisler proposed the metaphors of "infinitesimal microscope" and "infinite telescope". If one focuses an "infinitesimal microscope", say at the number 1, and magnifies by an infinite amount H, then one sees points that are an infinitesimal distance ε apart. On the other hand, if one focuses an "infinite telescope" at H, then one sees infinite numbers on the ordinary real scale. As such, in the neighborhood of any real number, NSA defines the existence of a cloud or galaxy of infinitesimals that can be treated as finite numbers for the purpose of manipulations. In NSA the limit process is built-in into the standard algebraic manipulations of hyperreal numbers. As a result, a discontinuous function, such as friction force, can be rigorously represented by a continuous hyperreal approximation that is infinitely close to the actual discontinuous function. The NSA approach enables one to use the conventional numerical simulation to consistently and reliably predict the behavior of systems involving discontinuous forces.

Batty et al. [16] have proposed using a line segment with an infinite hyperreal slope to represent the signum function. This representation of the signum function works quite well in problems that do not involve differentiation of the signum function itself. Farassat et al. [17] have given an excellent introduction to the basics of the NSA and have used it to investigate the resonance phenomenon in a simple spring–mass system subjected to harmonic excitation.

Here, as an example of a system involving discontinuous forces, a simple frictional system subjected to both harmonic as well as discontinuous excitations is considered. First, through NSA, the discontinuous friction force is replaced by a continuous hyperreal representation. Then, for the case of harmonic excitations, the Runge–Kutta method coded in Wolfram's Mathematica [18] is used to evaluate the solution. Point-wise, this solution is essentially identical to the corresponding analytical solution as given by Den Hartog [19]. For the case of discontinuous excitation, first a set of orthogonal tracking functions is introduced. Then, an equivalent analytical representation of the discontinuous excitation is developed through expansion in a series of these tracking functions. Using NSA, this excitation, which involves a finite number of discontinuities, is rigorously represented by continuous hyperreal approximations. Subsequently, the Runge–Kutta method is used to evaluate the solution. The main source of discontinuity in the dynamic system considered here is purely friction. However, NSA can be applied for dynamic systems in which the discontinuous effects are due to impact, shock, phase change, etc.

2. Formulation

The equilibrium equation for the single degree of freedom system in Fig. 1 is

$$mu'' + cu' + ku + F_s + F_d = P(t), \tag{1}$$

where m is the mass, c is the viscous damping coefficient, k is the spring stiffness, $P(t)$ is the applied load, u is the displacement response, and prime denotes differentiation with respect to time, t. Using a Coulomb model, the kinetic friction force, F_d, is given by

$$F_d = \mu_d mg \,\mathrm{Sgn}\, u' = \gamma\mu_s mg \,\mathrm{Sgn}\, u', \tag{2}$$

where $\gamma = \mu_d/\mu_s$ denotes the ratio of the dynamic coefficient of friction, μ_d, to the static coefficient of friction, μ_s, g denotes the gravitational acceleration, and Sgn is the signum function. The maximum value of the static friction force, F_s, is equal to $\mu_s mg$, and its value is zero during any sliding phase, i.e., F_s and F_d are mutually exclusive. During any non-sliding phase, its value is given by

$$F_s = (P(t) - ku)N(Z)Q, \tag{3}$$

where

$$Z = k\delta\left(\frac{\mu_s mg}{k\delta} - \left|\frac{P(t)}{k\delta} - \frac{ku}{k\delta}\right|\right) \tag{4}$$

and $Z \geqslant 0$ is a necessary but not sufficient condition for sticktion. Further, the switching function $N(Z) = 1$ for $Z \geqslant 0$ and $N(Z) = 0$ for $Z < 0$. $Q = 1$ characterizes the zero crossing time of the velocity, u', and its value as a function of time can be defined by

$$Q = 1 - |\mathrm{Sgn}\, u'|. \tag{5}$$

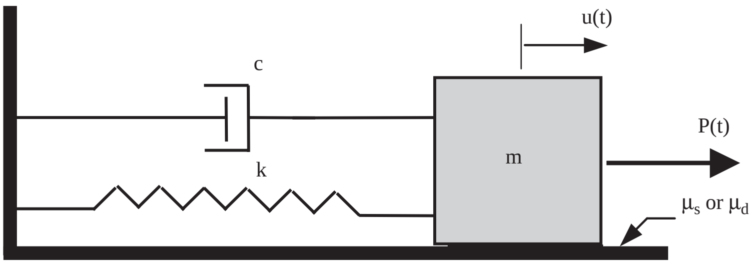

Fig. 1. Representation of a single-degree-of-freedom system.

It is necessary to have Q in Eq. (3) because F_s has to be zero when $u' \neq 0$. To non-dimensionalize the above relations, let

$$u = \delta y, \tag{6}$$

$$\tau = \omega t \;\Rightarrow\; u' = \omega\,\delta\dot{y} \;\Rightarrow\; u'' = \omega^2\delta\ddot{y}, \tag{7}$$

where dot denotes differentiation with respect to the non-dimensional time, τ, and $\omega = \sqrt{k/m}$. δ in Eq. (4) represents that magnitude of deformation in the spring at which the magnitude of the spring force, $k\delta$, is equal to the maximum value of the static friction force, $\mu_s\, mg$. Therefore,

$$\frac{\mu_s\, mg}{k\delta} = \frac{\mu_s g}{\omega^2\delta} = 1. \tag{8}$$

Substitutions of relations (6)–(8) into Eqs. (1)–(5) yield

$$\ddot{y} + 2\varsigma\dot{y} + y + f_s + f_d = p(\tau), \tag{9}$$

where

$$p(\tau) = \frac{P(\tau)}{k\delta}, \quad z = \frac{Z}{k\delta} = 1 - |p(\tau) - y|, \quad q = 1 - |\mathrm{Sgn}\,\dot{y}|, \tag{10}$$

$$f_s = \frac{F_s}{k\delta} = (p(\tau) - y)N(z)q, \quad f_d = \frac{F_d}{k\delta} = \gamma\,\mathrm{Sgn}\,\dot{y}, \tag{11}$$

and the switching function, $N(z)$, as defined by Mostaghel [20], is given by

$$N(z) = 0.5(1 + \mathrm{Sgn}\,z)[1 + (1 - \mathrm{Sgn}\,z)]. \tag{12}$$

Substitution of relations (10) and (11) into Eq. (9) yields the non-dimensional equation of equilibrium as

$$\ddot{y} + 2\varsigma\dot{y} + y + (p(\tau) - y)N(z)(1 - |\mathrm{Sgn}\,\dot{y}|) + \gamma\,\mathrm{Sgn}\,\dot{y} = p(\tau) \tag{13}$$

with the initial conditions: $y(0) = y_0$, $\dot{y}(0) = \dot{y}_0$. If the load $p(\tau)$ is continuous, then the sources of discontinuity in the above equation would be in the terms of $\mathrm{Sgn}\,\dot{y}$ and $N(z)$, both of which are functions of dependent variables. But if $p(\tau)$ is discontinuous, then a discontinuous function of the independent variable, τ, would also be present. In the following, first the discontinuous terms, $\mathrm{Sgn}\,\dot{y}$ and $N(z)$, will be replaced by their corresponding equivalent continuous hyperreal functions, and then two examples, one with continuous $p(\tau)$ and the other with discontinuous $p(\tau)$, will be presented.

3. Representation of discontinuities

There are a number of continuous functions that can equivalently represent the discontinuous function $\mathrm{Sgn}\,\dot{y}$ to any degree of desired accuracy. Mostaghel and Davis [21] listed four of them. Here, using the NSA technique [15], it will first be shown that the hyperbolic tangent function $\tanh\,\alpha\dot{y}$ can rigorously represent $\mathrm{Sgn}\,\dot{y}$. Then, this representation of the signum function will be used in subsequent developments. Let $\alpha = 1/\varepsilon^2$, where ε^2 is a positive real number in the neighborhood of zero. The limits of the function $\tanh\,\alpha\dot{y}$ from the right and from the left as $\varepsilon \to 0$

are evaluated as follows:

$$\tanh_{\dot{y}\to\varepsilon^+} \frac{\dot{y}}{\varepsilon^2} = \mathrm{st}\left(\frac{\mathrm{e}^{\dot{y}}/\varepsilon^2 - \mathrm{e}^{-\dot{y}/\varepsilon^2}}{\mathrm{e}^{\dot{y}/\varepsilon^2} + \mathrm{e}^{-\dot{y}/\varepsilon^2}}\right) = \frac{\mathrm{st}(1-\mathrm{e}^{-2\dot{y}/\varepsilon^2})}{\mathrm{st}(1+\mathrm{e}^{-2\dot{y}/\varepsilon^2})} = \frac{1-\mathrm{st}(\mathrm{e}^{-2/\varepsilon})}{1+\mathrm{st}(\mathrm{e}^{-2/\varepsilon})} = 1, \tag{14}$$

$$\tanh_{\dot{y}\to\varepsilon^-} \frac{\dot{y}}{\varepsilon^2} = \mathrm{st}\left(\frac{\mathrm{e}^{-\dot{y}/\varepsilon^2} - \mathrm{e}^{\dot{y}/\varepsilon^2}}{\mathrm{e}^{-\dot{y}/\varepsilon^2} + \mathrm{e}^{\dot{y}/\varepsilon^2}}\right) = \frac{\mathrm{st}(\mathrm{e}^{-2\dot{y}/\varepsilon^2}-1)}{\mathrm{st}(\mathrm{e}^{-2\dot{y}/\varepsilon^2+1)}} = -\frac{1-\mathrm{st}(\mathrm{e}^{-2/\varepsilon})}{1+\mathrm{st}(\mathrm{e}^{-2/\varepsilon})} = -1. \tag{15}$$

"st" in the above expressions is a symbol in NSA representing the "standard part" of an expression. The ± 1 limits as $\varepsilon \to 0$ (but never $\varepsilon = 0$) in the above expressions establish that the function $\tanh \alpha \dot{y}$, in which $\alpha = 1/\varepsilon^2$, can equivalently represent the signum function $\mathrm{Sgn}\, \dot{y}$. Therefore,

$$\mathrm{Sgn}\, \dot{y} \approx \tanh \alpha \dot{y}. \tag{16}$$

In NSA ε^2 is a hyperreal infinitesimal, therefore $\alpha = 1/\varepsilon^2$ is a hyperreal infinite. As shown in Fig. 2, in this case, ε^2 can be interpreted as the absolute value of an impending non-dimensional velocity for a subsequent sliding phase. Therefore, the discontinuity in the interval $[-\varepsilon^2, \varepsilon^2]$, about the zero velocity, is replaced by a continuous hyperreal representation. Because of the nature of infinitesimals as defined in NSA, the right-hand sides of expressions (14) and (15) are hyperreal approximations. As such, the function $\tanh \alpha\dot{y}$ is infinitely close to the signum function. Similarly, $\mathrm{Sgn}\, z$ can be represented by

$$\mathrm{Sgn}\, z \approx \tanh \eta z, \tag{17}$$

where, like α, η is a hyperreal infinite.

It is noted that the right-hand side of expression (16) is not just a mere approximation to the left-hand side, as previously assumed by the author [21]. It is a rigorous mathematical representation. It is also noted that as $\varepsilon \to 0$, the function $\tanh \alpha\dot{y} \to \mathrm{Sgn}\, \dot{y}$ at the much higher rate of $1/\varepsilon^2$.

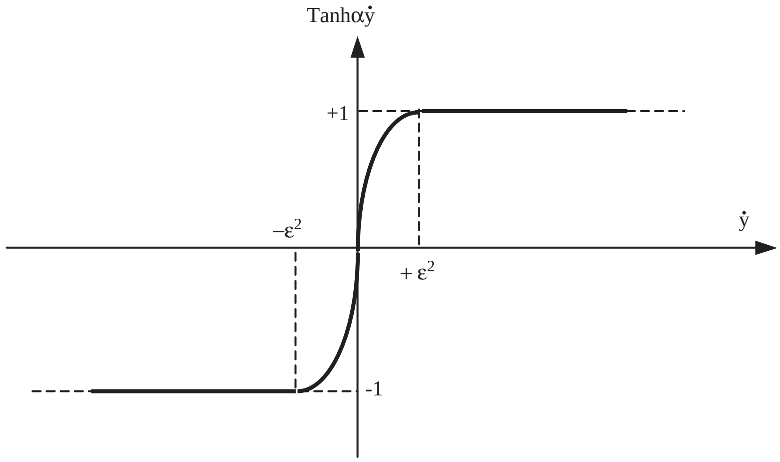

Fig. 2. A representation of the signum function $\mathrm{Sgn}\, \dot{y} = \dot{y}/|\dot{y}| \approx \tanh \dot{y}/\varepsilon^2 = \tanh \alpha\dot{y}$.

4. Examples

4.1. Continuous excitations

As the first example, consider a case for which the continuous excitation, $p(t)$, is harmonic. Therefore,

$$p(\tau) = p_0 \sin \Omega\tau = p_0 \sin \frac{\Omega}{\omega}\tau = p_0 \sin \beta\tau, \tag{18}$$

where Ω is the forcing frequency and $\beta = \Omega/\omega$ denotes the frequency ratio. Therefore, substitutions of relations (16)–(18) into the equilibrium equation (13) yield

$$\ddot{y} + 2\varsigma\dot{y} + y + (p(\tau) - y)N(z)(1 - |\tanh \alpha\dot{y}|) + \gamma \tanh \alpha\dot{y} = p_0 \sin \beta\tau, \tag{19}$$

where

$$N(z) = 0.5(1 + \tanh \eta z)[1 + (1 - \tanh \eta z)] \tag{20}$$

and z is defined in relations (10). As an example, consider a case for which $y(0) = 0$, $\dot{y}(0) = 0$, $\varsigma = 0$, $\gamma = \mu_d/\mu_s = 0.75$, $p_0 = 1.2$, and $\beta = 0.50$. Using the Runge–Kutta method coded in Mathematica [18], Eq. (19) is integrated numerically using sufficiently large values for α and η. Very large values of α and η require increased computational effort and can introduce convergence problems. For the system considered, values of α and η of the order of 10^2 yield solutions that satisfy Eq. (19) point-wise in time. Using values of the order 10^3 or 10^4 yields solutions essentially identical to the ones obtained using values of the order 10^2. However, for simulation of each system, the sensitivities of α and η to the variations in the system's parameters as well as the excitation frequency should be investigated.

The non-dimensional response quantities are presented in Figs. 3–7. Fig. 4 shows that the sticktion force, f_s, is zero for the intervals of time during which the velocity is not zero. It also shows that when the velocity is zero, f_s varies with time. On the other hand, Fig. 5 shows that the

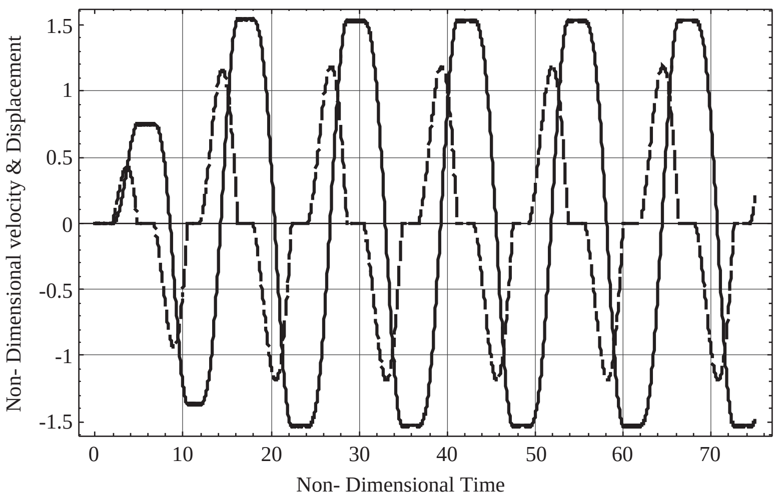

Fig. 3. Velocity and displacement response ($\dot{y}$, – – –; y,——).

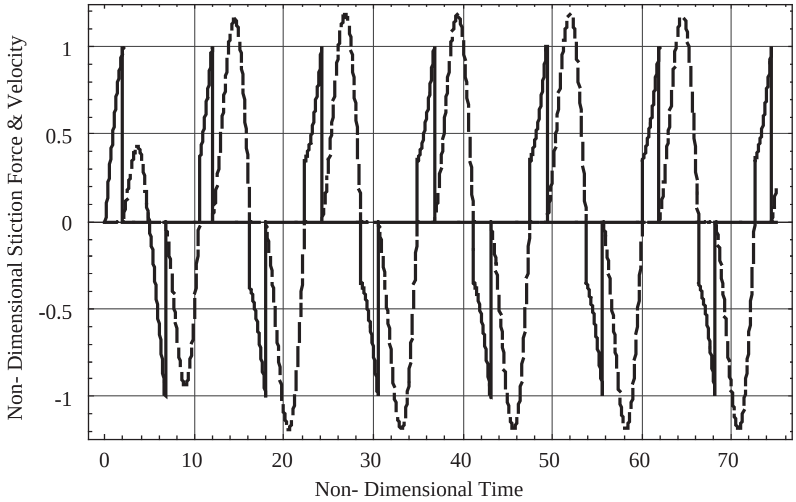

Fig. 4. Velocity and stiction force ($\dot{y}$, – – –; f_s, ——).

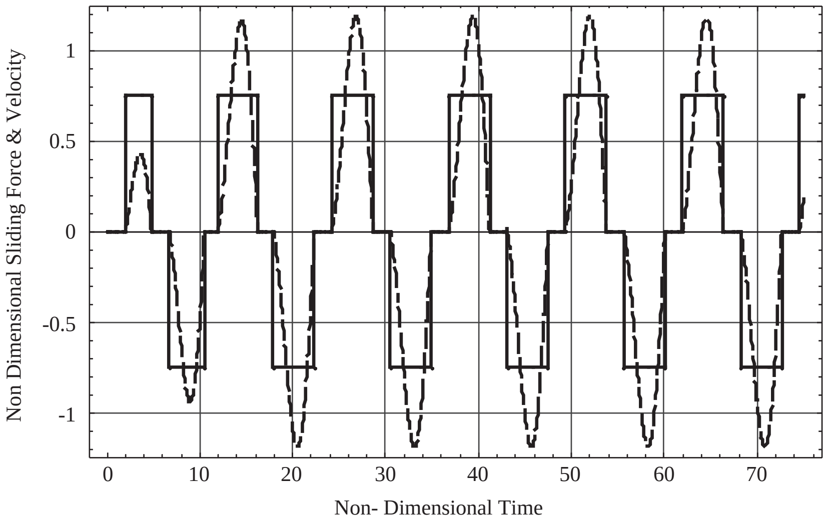

Fig. 5. Velocity and kinetic friction force ($\dot{y}$, – – –; f_d, ——).

kinetic friction force, f_d, is constant during sliding phases and is zero during sticktion phases. Fig. 6 is the phase diagram depicting the fact that, for the given parameters, the response very quickly becomes periodic. Fig. 7 shows the force–displacement relation that is typical for frictional systems. The spikes in this figure represent the transition points between sticktion and sliding phases. Since the specified dynamic coefficient of friction is equal to 75% of the value of the static coefficient of friction, the maximum value of the friction force develops a jump at the transition points. This fact can also be observed by a comparison of Figs. 4 and 5.

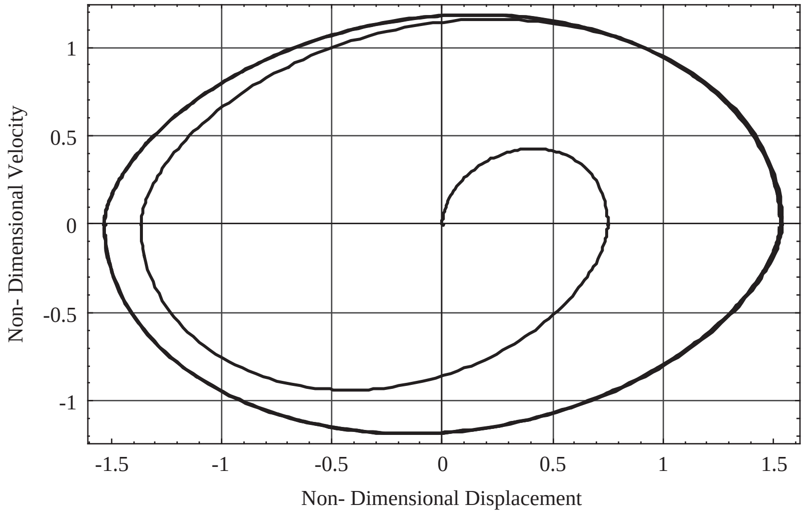

Fig. 6. Variation of velocity with displacement.

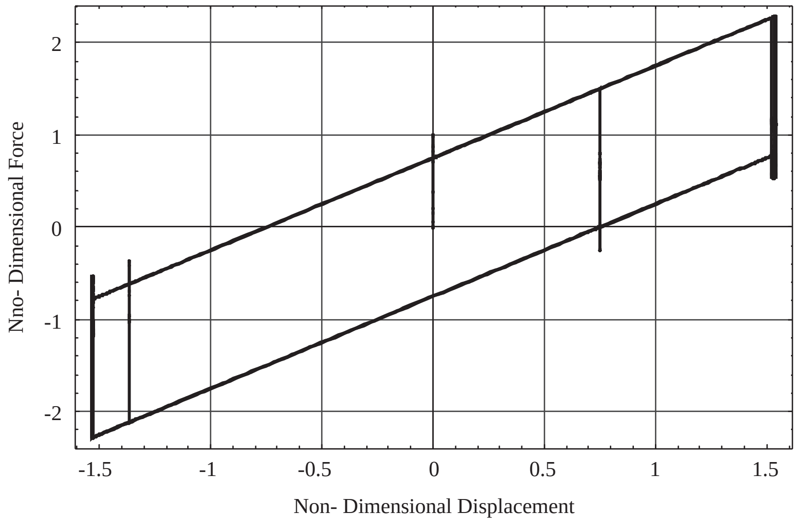

Fig. 7. Force–displacement response, continuous input.

4.2. Discontinuous excitations

As the second example, consider a case for which the discontinuous excitation, $p(\tau)$, is as given in Table 1. The time history for $p(\tau)$ is shown in Fig. 8. To express $p(\tau)$ as an equivalent continuous function of time, let the switching functions be defined by

$$N(w_i) = 0.5(1 + \mathrm{Sgn}\, w_i)[1 + (1 - \mathrm{Sgn}\, w_i)], \tag{21}$$

Table 1
Time history of the discontinuous excitation

τ_i	0	5	15	20	35	50	55	65	75
p_i	+1.25	−1.25	+1.25	−2.00	+2.00	−1.25	+1.25	−1.25	−1.25

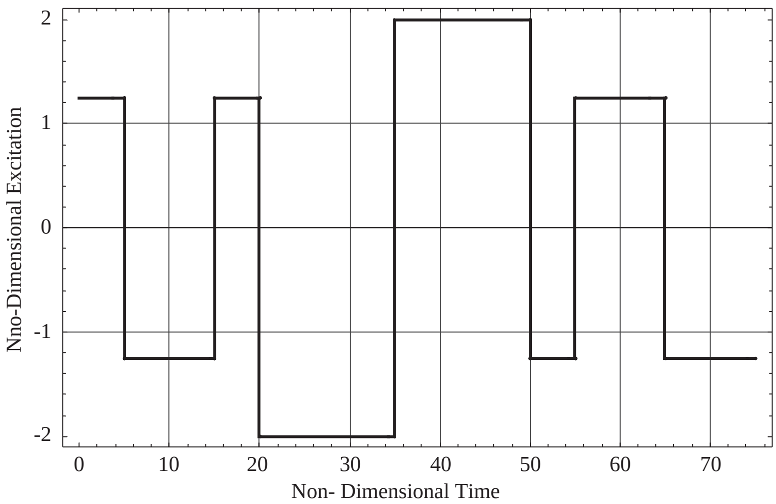

Fig. 8. Time history of the excitation.

where $w_i = \tau - \tau_i$ and $\mathrm{Sgn}\, w_i$ is defined by the following continuous representation:

$$\mathrm{Sgn}\, w_i \approx \tanh[\lambda(\tau - \tau_i)], \tag{22}$$

where $\tau_i = \omega t_i$ and λ is a hyperreal infinite.

In order to analytically represent the discontinuous excitation $p(\tau)$, consider the tracking function,ϕ_i, as defined by Mostaghel and Byrd [22]:

$$\phi_i = N(w_i) - N(w_{i+1}), \tag{23}$$

where $N(w_{n+1}) = 0$. As defined in the above equation, the functions ϕ_i, where $i = 1, 2, \ldots, n$ form an orthogonal set of functions, i.e., $1/(\tau_{i+1} - \tau_i) \int_{\tau_i}^{\tau_{i+1}} \phi_i * \phi_j \, \mathrm{d}\tau = 0$ for $i \neq j$ and $1/(\tau_{i+1} - \tau_i) \int_{\tau_i}^{\tau_{i+1}} \phi_i * \phi_j \, \mathrm{d}\tau = 1$ for $i = j$. Therefore, the discontinuous function, $p(\tau)$, can be expanded in a series of these orthogonal functions and can be expressed analytically by the series

$$p(\tau) = \sum_{i=1}^{n} \phi_i \, p_i(\tau), \tag{24}$$

where $p_i(\tau)$represents the function $p(\tau)$ in the interval $\tau_i \leqslant \tau < \tau_{i+1}$. The only condition on $p_i(\tau)$ is that it must be continuous in the interval $\tau_i < \tau < \tau_{i+1}$. Substituting the above representation of the excitation into Eq. (13) yields the equilibrium equation as

$$\ddot{y} + 2\varsigma\dot{y} + y + (p(\tau) - y)N(z)(1 - |\tanh \alpha\dot{y}|) + \gamma \tanh \alpha\dot{y} = \sum_{i=0}^{n} \phi_i p_i(\tau). \tag{25}$$

As an example, let $y(0) = 0$, $\dot{y}(0) = 0$, $\varsigma = 0$, $\gamma = \mu_d/\mu_s = 0.75$, which are the same values as in example 1. Numerical integration of Eq. (25) yields the non-dimensional response quantities that are presented in Figs. 9–13. As in the case of continuous excitations, Fig. 10 shows that the

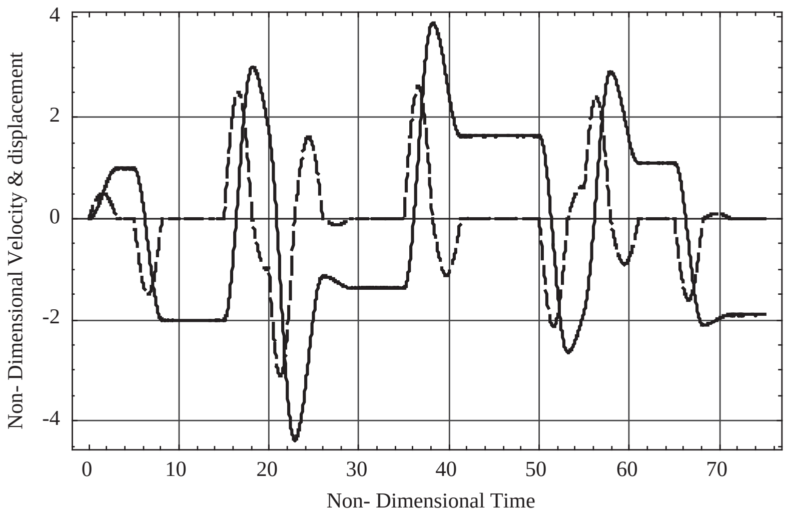

Fig. 9. Velocity and displacement response ($\dot{y}$, – – –; y,——).

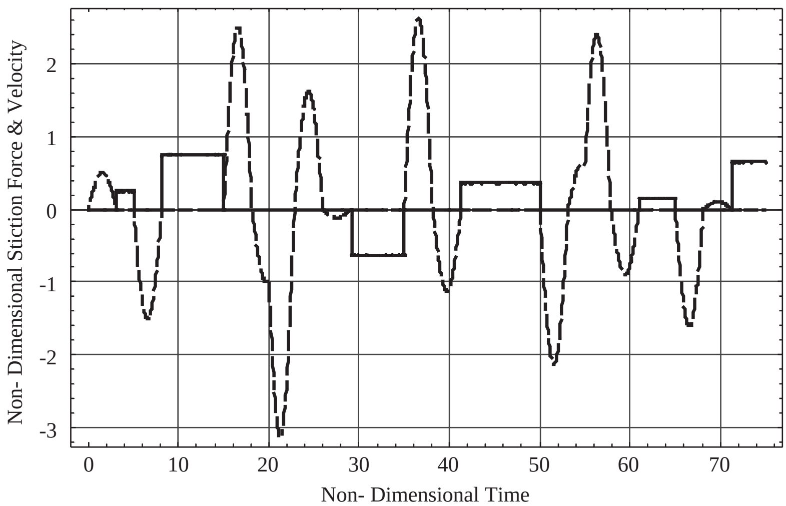

Fig. 10. Velocity and stiction force ($\dot{y}$, – – –; f_s,——).

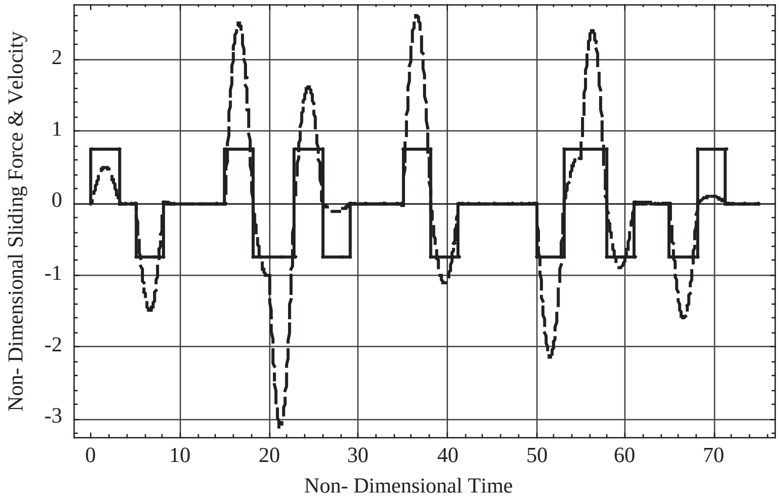

Fig. 11. Velocity and kinetic friction force ($\dot{y}$, – – –; f_d,——).

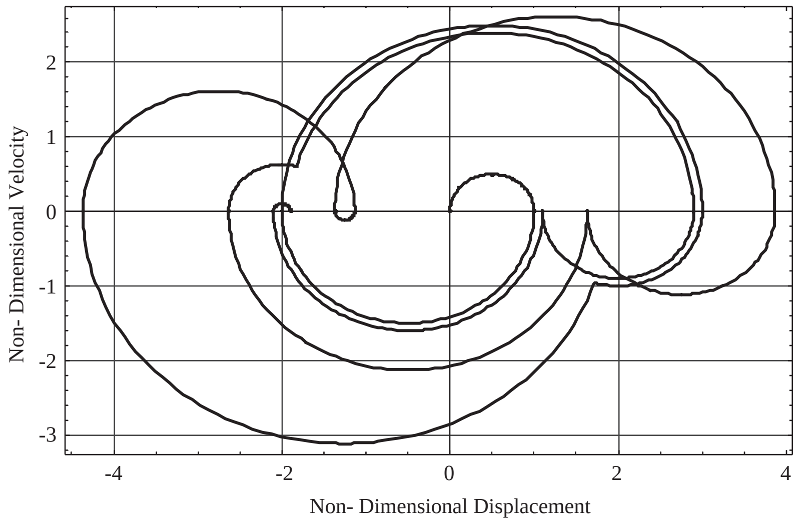

Fig. 12. Variation of velocity with displacement.

sticktion force, f_s, is zero for the intervals of time during which the velocity is not zero. It also shows that during the times when the velocity is zero, f_s has non-zero values. On the other hand, Fig. 11 shows that the kinetic friction force, f_d, is constant during sliding phases and is zero during sticktion phases. Fig. 12 represents the phase diagram. Fig. 13, similar to Fig. 7, shows the force–displacement relation typically expected for frictional systems.

The solution of Eq. (25) is far more sensitive to the values of α and η than is the solution of Eq. (19). For the system considered, to satisfy Eq. (25) at all points in time, one needs to use values for α and η of the order of 10^6, and for λ of the order of 10^{10}.

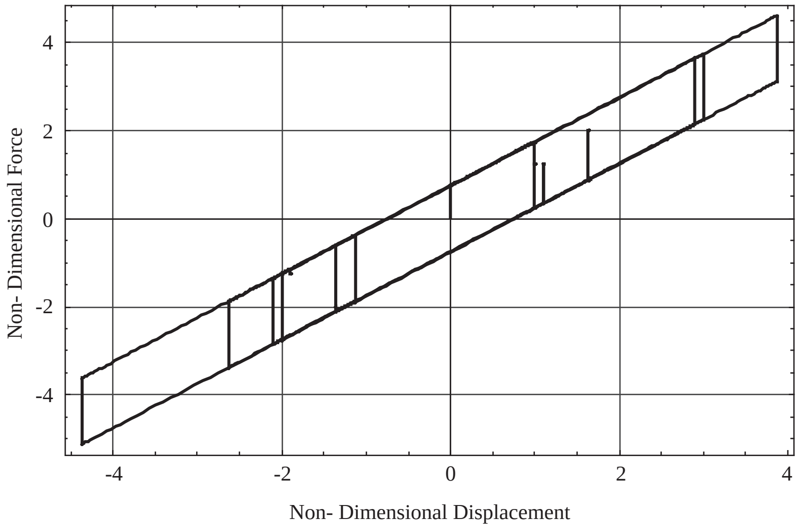

Fig. 13. Force–displacement relation, discontinuous input.

5. Summary and remarks

To consistently simulate systems involving discontinuous forces, two new schemes are introduced. In the first scheme, the NSA is used to replace discontinuous functions with continuous representations. In the second scheme, a set of orthogonal tracking functions is defined and used to analytically express a discontinuous function in a series. As examples of the efficacy of these schemes, the responses of a simple frictional system subjected to both a continuous as well as to a discontinuous excitation are evaluated. In the case of continuous excitation, the response quantities are essentially identical to those from the available analytical solution. The system's sensitivity to perturbations dictates how small an infinitesimal (like the ε used in this investigation) should be. The best test of the resulting solution is the point-wise satisfaction of the equilibrium equation to the desired level of accuracy. It should be noted that, in the given examples, since both Sgn $\dot{y}$ and Sgn z are functions of the dependent variables, identical values are used for α and η. Neither example is very sensitive to the selection of η. For the system considered, the solutions are essentially identical for η as small as 10^2. For the first example, i.e. continuous input, α as low as 10^2 and as high as 10^5 yield essentially identical solutions. On the other hand, for the case of discontinuous excitation, the solution is very sensitive to the values of α and λ. For simulation of any system, the sensitivities of α and η to the variations in the system's parameters as well as the type of excitation should be investigated.

References

[1] D.K. Nims, P.J. Richter, R.E. Bachman, The use of the energy dissipating restraint for seismic hazard mitigation, *Earthquake Spectra* 9 (1993) 467–489.

[2] J. Inaudi, J. Kelly, Dynamics of homogeneous frictional systems, in: A. Guran, F. Pfeiffer, K. Popp (Eds.), *Dynamics with Friction: Modeling, Analysis, and Experiment*, World Scientific, London, 1996, pp. 93–136.

[3] A.S. Mokha, M.C. Constantinou, A.M. Reinhorn, Verification of friction model of teflon bearings under triaxial load, *Journal of Structural Engineering* 119 (1) (1993) 240–261.

[4] N. Mostaghel, M. Khodaverdian, Seismic response of structures supported on R-FBI system, *Journal of Earthquake Engineering and Structural Dynamics* 16 (6) (1998) 839–854.

[5] G. Ahmadi, F.C. Fan, M.N. Noori, A thermodynamically consistent model for hysteretic materials, *Iranian Journal of Science and Technology Transactions B* 21 (3) (1997) 257–278.

[6] F.C. Fan, G. Ahmadi, I.G. Tadjbakhsh, Multistory base-isolated buildings under a harmonic ground motion—part I: a comparison of performances of various systems, *Nuclear Engineering and Design* 123 (1990) 1–16.

[7] J.H. Wang, Design of a friction damper to control vibration of turbine blades, in: A. Guran, F. Pfeiffer, K. Popp (Eds.), *Dynamics with Friction: Modeling, Analysis, and Experiment*, World Scientific, London, 1996, pp. 169–195.

[8] B. Armstrong-Helouvry, P. Dupont, C. Canudas De Wit, A survey of models analysis tools and compensation methods for the control of machines with friction, *Automatica* 30 (7) (1994) 1083–1138.

[9] Y. Wang, An analytical solution for periodic response of elastic-friction damped systems, *Journal of Sound and Vibration* 189 (3) (1996) 299–313.

[10] B. Blazejczyk-Okolewska, K. Czolczynski, T. Kapitaniak, J. Wojewoda, *Chaotic Mechanics in Systems with Impact and Friction*, World Scientific, London, 1999.

[11] W. Rzymowski, Existence of solutions for a class of discontinuous differential equations in R^n, *Journal of Mathematical Analysis and Applications* 233 (1999) 634–643.

[12] A.F. Filippov, *Differential Equations with Discontinuous Righthand Sides*, Kluwer Academic Publishers, Dordrecht, Netherlands, 1988.

[13] M.F. Danca, S. Coreanu, On a possible approximation of discontinuous dynamical systems, *Chaos, Solutions and Fractals* 13 (2002) 681–691.

[14] A. Robinson, *Non Standard Analysis*, North-Holland, Amsterdam, 1966.

[15] H.J. Keisler, *Elementary Calculus, An Infinitesimal Approach*, Prindle, Weber & Schmidt, Boston, 1986.

[16] R.S. Baty, M.R. Vaughn, F. Farassat, A nonstandard analysis of a simple discontinuous force equation modeling continuous motion, *Journal of Sound and Vibration* 202 (2) (1997) 288–297.

[17] F. Farassat, M.K. Myers, A simple application of nonstandard analysis to forced vibration of a spring-mass system, *Journal of Sound and Vibration* 195 (2) (1996) 340–345.

[18] S. Wolfram, *The Mathematica Book*, Cambridge University Press, Cambridge, 1999.

[19] J.P. Den Hartog, Forced vibrations with combined coulomb and viscous friction, *American Society of Mechanical Engineers* 53 (1931) 107–115.

[20] N. Mostaghel, Analytical description of pinching, degrading hysteretic systems, *Journal of Engineering Mechanics* 125 (2) (1999) 216–224.

[21] N. Mostaghel, T. Davis, Representations of coulomb friction for dynamic analysis, *Earthquake Engineering and Structural Dynamics* 26 (5) (1997) 541–548.

[22] N. Mostaghel, R.A. Byrd, Inversion of Ramberg–Osgood equation and description of hysteresis loops, *International Journal of Non-Linear Mechanics* 37 (2002) 1319–1335.